REWETTING AND BOILING IN WATER JET IMPINGEMENT ON HIGH TEMPERATURE STEEL SURFACE*

H. Leocadio[1]
C. W. M. van der Geld[2]
J. C. Passos[3]

Abstract
For the first time, high-speed imaging (20 kfps) from the boiling phenomenon within water jet impingement zone during quenching of a high temperature (300°C - 900°C) steel plate was observed. The inverse heat conduction method gave the heat flux and the temperature at the plate surface from temperatures measured with thermocouples inserted into the plate. Surprisingly, gas bubbles, from a degassing process, on top of a thin vapor film have been observed. Surface roughness induces the occurrence of rewetting on surface temperatures above the critical point of water. For an initial surface temperature of 300°C, rewetting phenomenon took place without occurrence of vapor film, but for surfaces at or above 450°C, even in very high jet subcooling of 80K, vapor film formation was observed. In spite of high subcooling and velocity of jet, an intense vapor bubble activity was observed within wet region and ceased at surface temperature of 246°C for subcooling of 80K. Temperature and time of rewetting are strongly affected by the initial surface temperature and jet subcooling and, less intensely, by jet velocity.

Keywords: Degassing; Boiling, Rewetting; Quenching of steel; Jet impingement.

[1] *MSc, Specialist researcher, R & D Center, Usiminas Steel, Ipatinga, MG, Brazil.*
[2] *PhD, Professor, Department of Chemical Engineering, Eindhoven University of Technology, Netherlands.*
[3] *Dr, Professor, Department of Mechanical Engineering, Federal University of St Catarina, Brazil.*

** Technical contribution to the 55º Seminário de Laminação e Conformação de Metais, part of the ABM Week, October 2nd-4th, 2018, São Paulo, SP, Brazil.*

1 INTRODUCTION

Water jet impingement quenching has high cooling potential and it is used as an effective mean of cooling in many industrial applications involving rapid cooling, such as, emergency core cooling in nuclear power plants and power dissipation in the micro-electro-mechanical devices. Steel industries widely employ it for accurate temperature control, which ensures the mechanical and metallurgical properties, where the surface temperature (800–1100°C), heat flux (above 6 MW/m²) and cooling rate (above 100°C/s) are typically very large and acceptable cooling times are relatively short. The key factor for the rapid cooling during quenching is the rewetting process which occurs when the hot surface is cooled down to a temperature that allows a stable solid-liquid contact, referred as the rewetting temperature (T_{rw}). The maximum heat flux is achieved when the rewetting temperature is reached. Therefore, an efficient cooling control starts at the onset of rewetting. The accurate knowledge of rewetting temperature and, as well as, the time required to the rewetting take place (rewetting delay) are essential for enhanced of the quenching processes and the development in ultra-fast cooling technology.

The limit condition for water remains liquid is the critical temperature of 374°C and without undergoes instantaneous vaporization [1] is 325°C [2], at atmospheric pressure. However, a number of studies have reported rewetting taking place on surface temperature exceeding by far the critical point of water. Hall et al. [3] advised that high rewetting temperatures above 900°C, reported by Ishigai et al. [4] and Ochi et al. [5], and 710°C, by Filipovic et al. [6], in water jet quenching should be considered physically impossible, because greatly exceed the water critical point. Water jet quenching [7] and reflooding [8] studies concluded that rewetting can occur only on surface below 300°C and 308°C, respectively. Also, analytical studies [9, 10] calculated rewetting interface temperature ranging from 303°C to 325°C. All those results converge to rewetting temperature bellow critical point. On another hand, recent water jet quenching experiments [11, 12, 13, 14] reported rewetting surface above 700°C without film boiling formation, despite initial surface temperature (Ti) as high as 1000°C. Karwa & Stephan [15] reported rewetting temperature equal to 650°C for water jet at 25°C and the heat flux was above 6 MW/m² in wetted region without boiling activity. They argued that the jet velocity and subcooling can suppress the bubbly activity and rewetting surfaces in excess of the critical temperature of the liquid can be achieved.

Wang et al. [16] concluded from water jet (13-43°C) cooling experiments of a hot steel plate (200–900°C) that T_{rw} is severely affected by Ti and almost unaffected by velocity and temperature of the jet and a higher T_i leads to a higher T_{rw}. Contrary, Takrouri et al. [17] concluded Trw is not affected by T_i but it strongly dependent on jet temperature, from their investigation of water jet (15-80°C) quench of (380–780°C) horizontal tubes. Piggott et al. [18] and Mozumder et al. [19] found the rewetting delay (t_{rw}) as a strong function of T_i, jet subcooling and velocity, but for subcooling higher than 30K the delay is nonexistent [18]. Contrary, Wang et al. [16] reported t_{rw} is unaffected by T_i, jet subcooling and velocity in impingement region. For Agrawal et al. [13] jet velocity has no influence on rewetting delay but it affects rewetting temperature. According to the literature above mentioned, ambiguities and contradictions do exist among researchers and the boiling phenomenon in the jet impingement quenching remain unknown.

2 MATERIAL AND METHODS

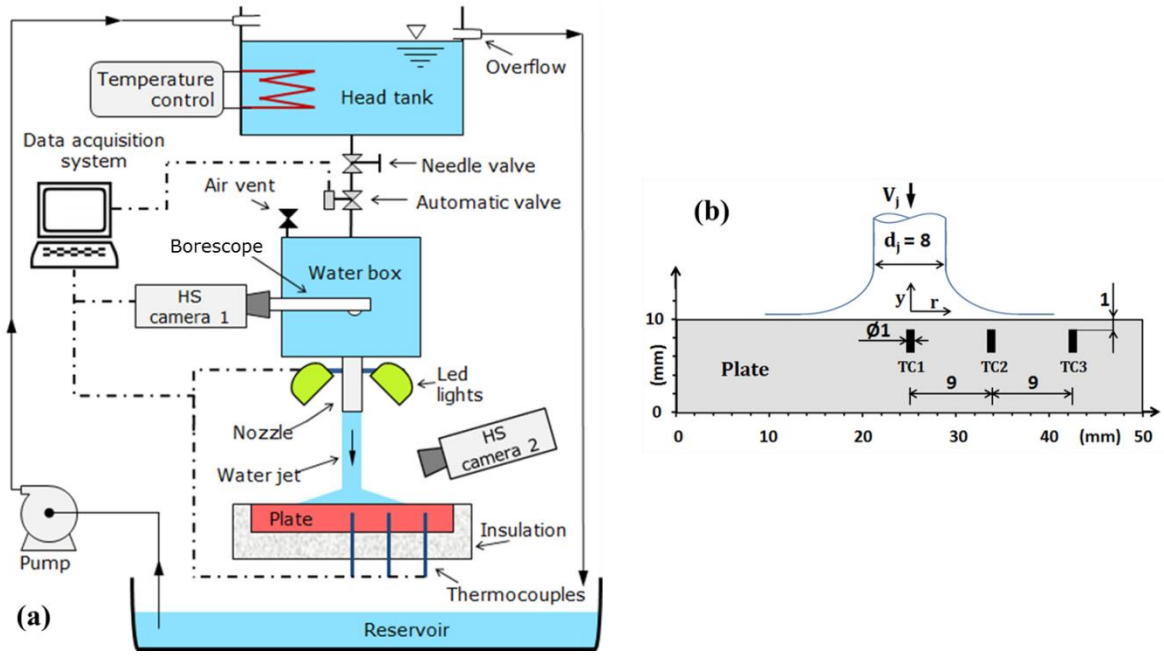

Figure 1. (a) Schematic of the test rig; (b) Schematic of cross section jet impinging on test plate with thermocouples (TC1, TC2, TC3) located in line at radial positions (r).

The main components of the experimental setup is outlined in Figure 1-a. Ordinary city water was stored in an open head tank and the desired water temperature was maintained by a thermostat controller. The pump sends water from reservoir to the head tank. The overflow tube kept constant the water level in the head tank, assuring a constant pressure in box and a stable jet at nozzle exit, which was located centrally at 40 mm above the test plate surface. The inner diameter of nozzle is 9.7 mm. The borescope is connected to the objective lens of the high-speed video camera #1 while the viewer was inserted into the water box. The borescope viewer was positioned centrally above the hole of nozzle exit in manner not disturb the water jet stability and to allow recording imaging through the water jet, yielding top views from the jet impingement zone. High-speed camera #1 captured images at range of 5 to 20 kfps. The high-speed camera #2 captured external images by side of the jet at 300 fps. A series of LED lights surrounding the nozzle exit supply enough lighting to record the inner events at impingement zone. The water flow rate is set by needle valve. Figure 1-b shows the cross section of a jet of 8 mm impinging on test plate of 50 x 50 x 10 mm³. The impinging jet diameter is similar those used in hot strip mill cooling. The test plate material was the type 304 stainless steel (SS) which produces protective chromium oxide (chromia) layer against high temperature oxidation to avoid the formation of peeling of oxide scale and the heat generation that occurs in carbon steel which distracts the temperature reading. On the plate sides without water impingement, insulation with low thermal conductivity of 0.11 W/(m.K) at 800°C and 25 mm thick was used. Three holes of 1.1 mm and 9 mm depth were drilled and checked by calipers. The thermocouples TC1, TC2, and TC3 are located in line at radial positions of 0, 9 and 18 mm, respectively, from the center of plate at depth of 1 mm below the top surface. Grounded thermocouples Type-K, 1 mm in sheath diameter made of 304 SS (the same as test plate), was used. High temperature thermal paste with conductivity of 70 W/(m.K) was inserted into the hole to insure good thermal thermocouple-plate contact.

The test plate was heated by a manual electrical oven (3 kW) at test quenching position. The data acquisition system simultaneously triggers the automatic valve, the high-speed camera, LED lights and acquires and stores the data. The plate temperature history during cooling process was measured by three thermocouples inserted into the test plate at rate of 50 Hz. The test plate was heated 50°C beyond the initial test temperature. The quenching tests were carried out at T_i of 300, 450, 600, 750, and 900°C which are commonly used in hot strip mill cooling. The water was heated up by electrical heater and recirculated through head tank, water box and reservoir until reach the desire test temperature. The jet temperatures were 20°C, 50°C and 70°C (subcooling of 80K, 50K and 30K) with velocities of 1 and 3 m/s. Before each experiment, the impinging surface was sanded with 320 grit sandpaper and cleaned with acetone. The measured arithmetic mean roughness (Ra) at impingement zone surface, after quenching test, was found ranging 0.11 to 0.18 µm. For the new plate surface Ra = 0.10 µm. Calculated uncertainty was within 95% limits and was analyzed according to criteria suggested by Taylor [21] taking into account errors in measurement, calibration, machining, and measuring devices. Combining the uncertainties of thermocouple and data acquisition system, the uncertainty of temperature was ± 0.30%. The calculated relative uncertainty for heat flux (q) was ± 5 %.

The temperature history registered by thermocouples was used to predict the unknown heat flux and temperatures on the quenching surface. To estimate the heat flux and temperature distribution along the quenching surface, a successfully applied [22, 23, 24] commercial inverse heat conduction software, INTEMP, was used. The thermal properties of material can vary with temperature for each finite element. This is important since in quench experiment the temperature changes severely and avoids the large errors about 20% [25] in estimate heat flux when constant thermal property is used.

3. RESULTS AND DISCUSSION

3.2. Rewetting on high-temperature surface

Rewetting on surface temperature above critical point of 374°C is showed in Figure 2 for a plate at T_i = 896°C, V_j = 1 m/s, and T_j = 20°C. The rewetting process is explained in the stages I to IV. The sketches "a" and "d" provide an interpretation of the phenomena observed in photographs "b" and "c", based on the movie, which warrants easy interpretation. After application of water jet (t = 0) on hot surface part of the water becomes vapor and a film boiling starts immediately. Over time at t = 0.12 s (Stage I-a) the surface temperature drops only 9°C (T_s = 887°C) due to the thermal insulation of film boiling. The side image of Stage I-b shows the vapor layer as a white disk, which is confirmed by the top view in Stage I-c. In the top view “c” (stage I) bubbles are discerned as white spots. Due to the facts that these bubbles never condense, while some coalesce, and that they all keep on moving hectically until they move out of the observed impingement zone, it is concluded that these bubbles consist of gas rather than vapor. As far as the authors know, this is the first time such phenomenon was visualized during quenching.

The film boiling was observed during 0.21 s for jet subcooling of 80K. This makes clear that direct observation through the impinging jet is quite elucidating. After 0.21s (stage II-c), rewetting starts at the center of the impingement zone at T_s = 827°C, which is quite above the water critical point of 374°C. After the onset of rewetting, a rewetting front is formed (stage II-d) and the wetted area increases with time due to

the advancement of rewetting front (stage III-d) outwards. Nucleate boiling regime exists within wetted since rewetting has started while film boiling occurs outside the wetted area. The wetted area increases overtime due to the advancement of rewetting front outwards (stage III-d) until the impingement zone is completely wetted (stage IV-d). Many vapor bubbles growing and condensing were observed within wetted area (stage III-c), while outside of this area gas bubbles still remain on top of the film boiling, where T_s = 800°C. At t = 0.38 s only nucleate boiling regime exists (stage IV-c) in despite of high surface temperature of 703°C. Vapor bubbles with maximum diameters around 0.5 mm were observed, while the heat flux is about 6 MW/m². Out of the impingement zone (stage IV–b) the film boiling still exists and the wetted area continues to grow.

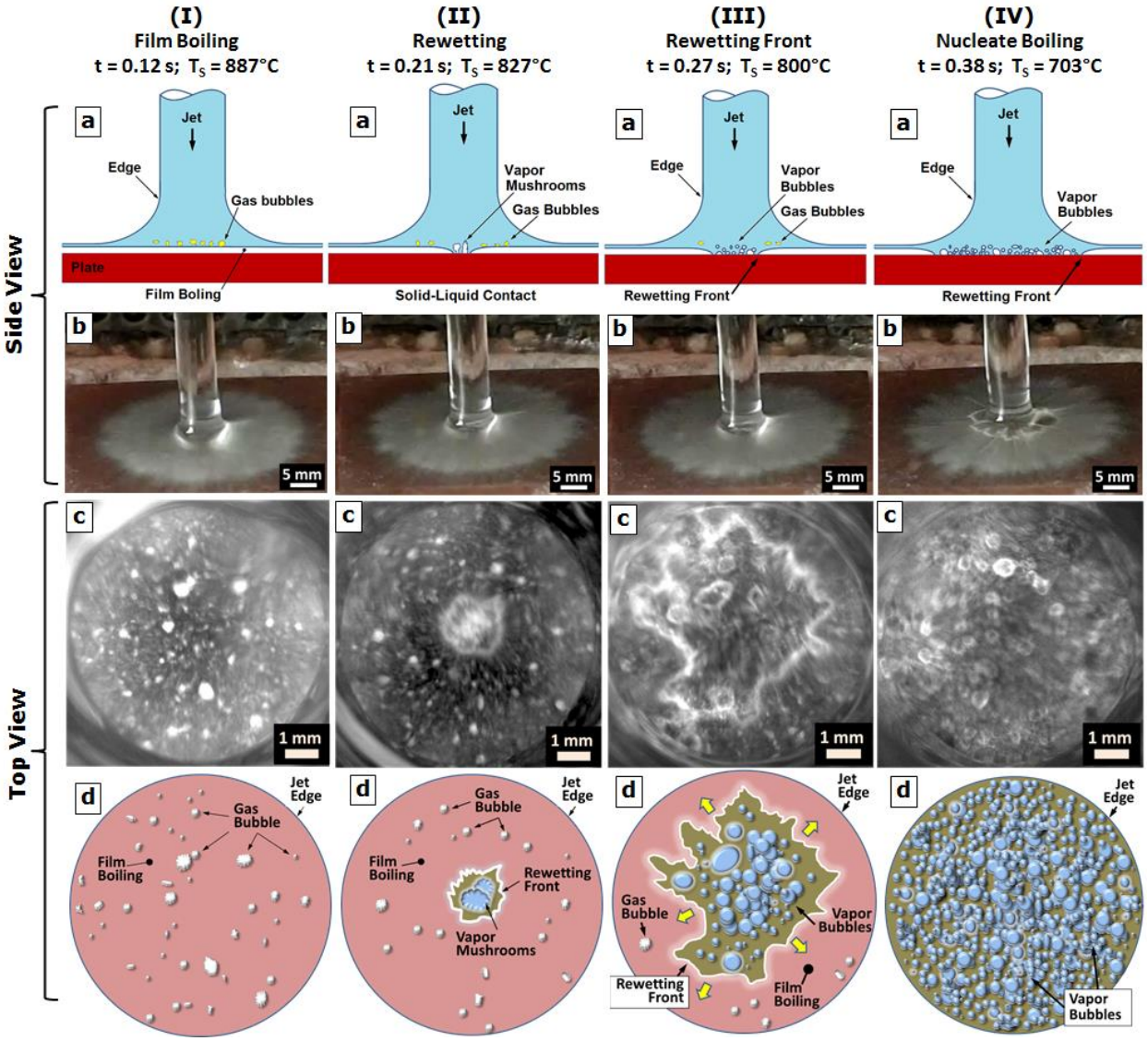

Figure 2. Images from top and side views of jet impingement zone during quench test (T_i = 896°C; T_j = 20°C; V_j = 1 m/s). Stages: (I) degassing on top of film boiling, (II) onset of rewetting, (III) rewetting front, and (IV) nucleate boiling.

Figure 3 shows the effects of T_i and jet subcooling (ΔT_{sub}) on rewetting temperature (T_{rw}) and rewetting delay time (t_{rw}). For a constant subcooling of 50K with T_i = 600°C and 750°C, t_{rw} = 0.08 s and 0.28 s and T_{rw} = 593°C and 656°C, respectively (see Figure 3-a & c). For a constant subcooling of 80K with T_i = 750°C and 896°C,

t_{rw} = 0.11 s and 0.21 s and T_{rw} = 738°C and 827°C, respectively (see Figure 3-b and d). An increase in ΔT_{sub} and/or T_i causes a raise in T_{rw}. An increase in ΔT_{sub} and/or reduction in T_i cause a decrease in t_{rw}. The occurrence of rewetting and nucleate boiling regime on surface temperatures above thermodynamic limit of water superheat (T_{tls}) and water critical point of 374°C was visually confirmed for all experiments with T_i = 450°C to 900°C. Figure 3 clearly show that rewetting may start anywhere and even at place out of the impingement zone (Figure 3-c). Figure 4 shows a test for T_i = 300°C and jet at 20°C. Stage I shows the jet touching down the surface and the rewetting occurring in the whole impingement zone immediately, without film boiling formation. A different behavior from those observed in Figure 3. After 2.8 ms (Stage II) the surface was wetted and a high bubbly activity was observed. This experiment suggests that rewetting is bound to occur on surface temperature below T_{tls}.

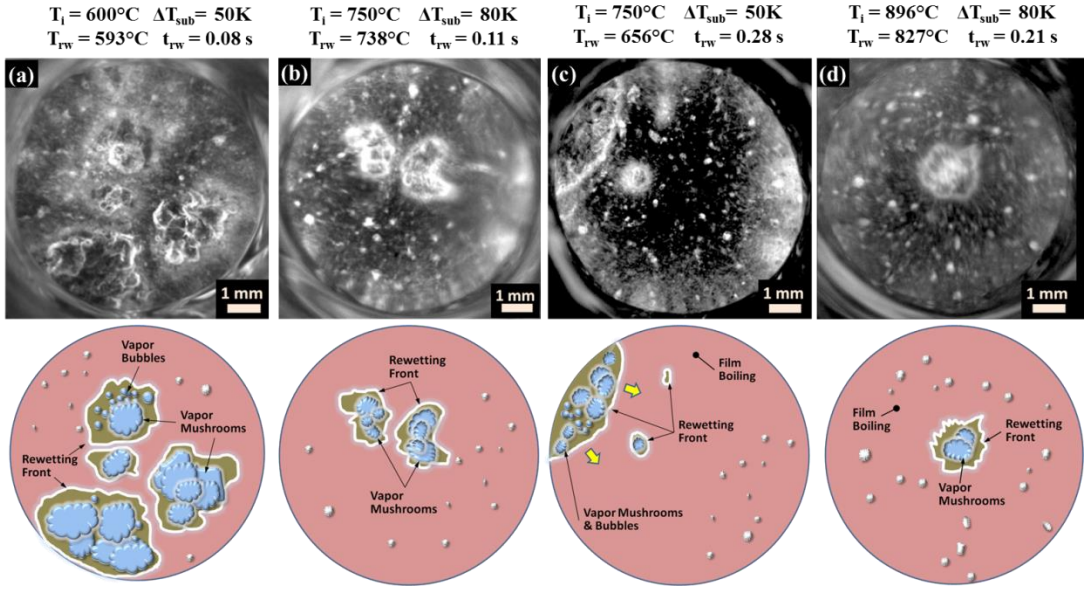

Figure 3. Top views images of rewetting for 600°C ≤ T_i ≤ 900°C, 50K ≤ ΔT_{sub} ≤ 80K, and V_j = 1 m/s.

Considering that roughness affects the rewetting phenomenon, when T_i = 300°C, everything on surface will be below T_{tls} allowing the rewetting to occur on whole surface instantly. However, if $T_i > T_{tls}$, then, firstly the liquid is repelled and, over time, rewetting starts anywhere on elevated points on surface which were firstly cooled below T_{tls} and became wet, as shown in Figure 3. This will be thoroughly examined in section 3.2.

3.2. Roughness for rewetting and boiling

Figure 5 explains the probable rewetting and boiling mechanism on surface temperatures above T_{tls}. Initially, steel plate, roughness and oxide have the same temperature above T_{tls} (Figure 5-a), then, when the water jet touches the hot surface the liquid is repelled and a film boiling is formed (Figure 5-a).Asperities can penetrate through the vapor layer and interacts with the subcooled water, but the asperity surface temperature is higher than T_{tls}, then, the liquid is repelled (Figure 5-a). Over time, the upper part of higher asperities is cooled below T_{tls}, allowing the rewetting (Figure 5-b) and change from film to nucleate boiling regime. Such asperities would

act as microfins removing heat (q) from hot surface to the liquid (Figure 5-b). This rewetting process spreads on vicinity asperities, then, more asperities would work as a fin reducing faster the surface temperature. This explains the high rewetting temperatures found in both present study and in the literature [16, 13]. Therefore, rewetting can start whenever any higher points on rough surface become wet.

The morphology and irregularity of a quenching surface, shown in Figure 5, can be better understood by the cross sections of a 900°C – plate quenched by a jet at 20°C, as shown in Figure 6. The surface is overlaid by a thin layer of chromium oxide of 1 – 2 µm, where peaks reach height of 4 µm (Figure 6-A). Roughness measurements found for peaks and valleys a total height roughness (Rt) of 5 µm. Figure 6-B shows cross-section of porous element on oxidized surface with height about 12 µm.

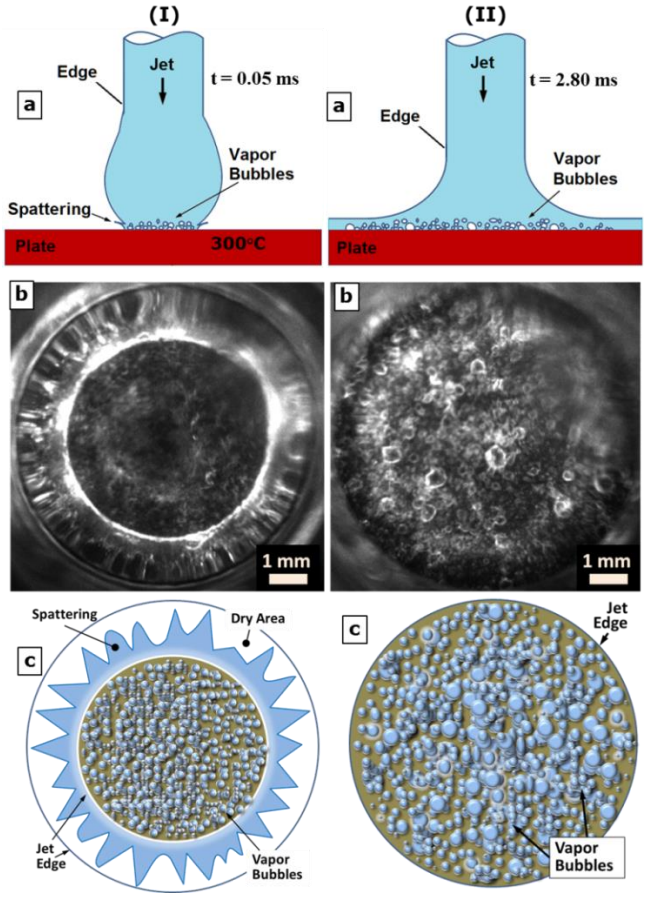

Figure 4. Quenching for T_i = 300°C and ΔT_{sub} = 80K, (a) jet touches the surface at 300°C without film boiling; (b) just 2.8 ms after jet collision.

Figure 7-A shows also a quenched surface (T_i = 900°C; T_j = 20°C) covered by chromia crystals and the presence of a large element of spongy texture with height about 30 µm. Figure 7-B shows the irregular surface with cavities due to chromia crystals. Therefore, since film boiling thickness ranges 3 – 5 µm [12] for a round jet of 10 mm at 20°C impinging on 1000°C-SS plate, the high and large particles and elements and/or peaks on surface, shown in Figure 6 to **Erro! Fonte de referência não encontrada.**, could easily penetrate through the thin vapor layer of 3 µm and interacts with the flowing liquid, consequently, starts the rewetting as explained in Figure 5. Since chromia has a very low thermal conductivity of 3.1 W/m.K, the temperature difference between the surfaces of chromia and steel during rewetting

condition was evaluated based on Biot number (Bi). If Bi < 0.1, then, the temperature gradient across chromia layer will be insignificant [20]. For initial surface temperature of 750°C and 900ºC and chromia layer thickness of 1 and 2 µm, the Biot number ranged from 0.00066 to 0.0022 and the temperature drop across the chromia layer ranged from 0.5°C to 2°C. Thus, chromia layer no act as thermal barrier since Bi << 0.1 and temperature drop was insignificant.

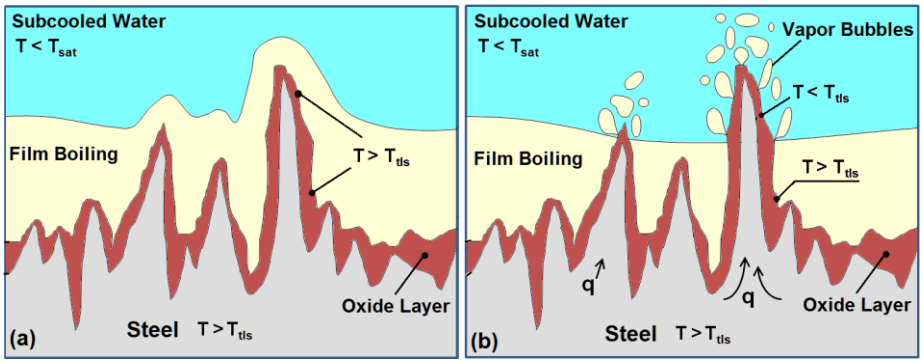

Figure 5. Schematic representation of rewetting and boiling induced by asperities.

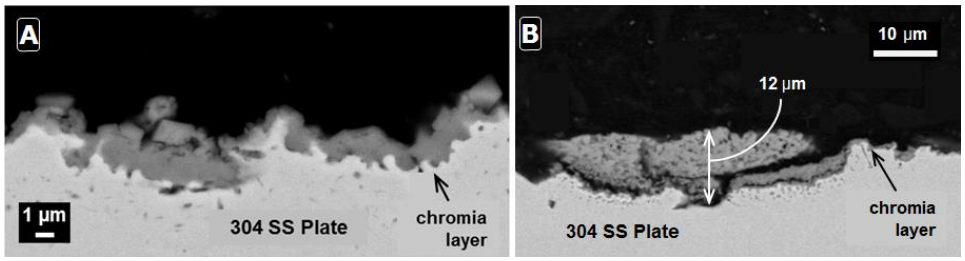

Figure 6. A) cross-section of the plate surface overlaid by chromium oxide layer with peak and valleys; B) cross-section of the plate surface overlaid by chromium oxide layer with the presence of a porous element 12 µm high.

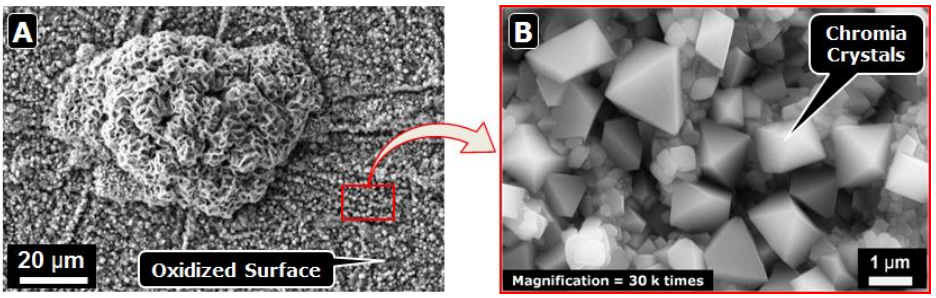

Figure 7. Surface morphology of quenched surface plate (T_i = 900°C; T_j = 20°C) covered by chromia crystals and the presence of a large element of spongy texture and (D) details of chromia crystals.

Figure 8 shows quenching tests for different surface conditions. For all tests rewetting started firstly where the surface was rougher (more rusty) and/or with high concentration of particles with highest elevated points on surface. Figure 10-a shows a surface with straight scribbles of graphite and corrosion spots (see red arrows on image the left hand side - LHS) before impingement of jet on surface at 450°C, set as t = 0. The white blurs surrounding the edge of the jet are reflections of the LED lights. The rewetting starts 9 ms later exactly on the corrosion spots and on the scribbles of graphite (see red arrows on central image), where surface was rougher with porous elements. Figure 8-b shows a surface at 600°C with dust smudges just after jet

impingement at time zero. Again, rewetting occurred exactly where roughness is highest. Figure 8-c shows rewetting occurring on corrosion spots (surrounded by a red dashed line on the LHS) for a surface at 900°C. The corrosion spots can be seen on central image. Therefore, rewetting on surface temperatures above critical point of 374°C is only possible due to existence of roughness and always starts in anywhere on higher points whenever they become wet, as shown in Figure 3.

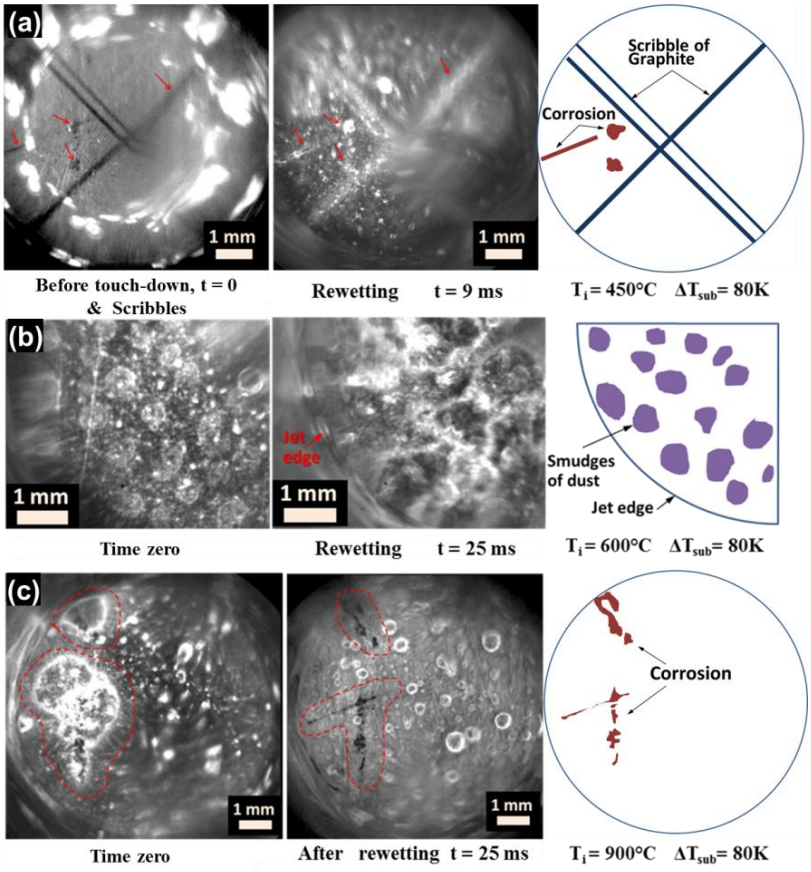

Figure 8. Images of the onset of rewetting firstly on rougher (more rusty) spot and/or highest elevated points on surface.

3.3. Rewetting temperature

Figure 9-a shows the experimental T_{rw} results plotted as a function of T_i = 450°C to 900°C, subcooling of 30K to 80K, and V_j = 1 and 3 m/s. For T_i = 450°C, the graphic shows symbols overlapped because rewetting always occurred at T_i, independent of subcooling and jet velocity. This suggests $T_{rw} = T_i$ when T_i is around 450°C. Until T_i = 600°C, T_{rw} is slightly affected by subcooling and non-affected by V_j. Hereafter till T_i = 900°C, the influence of subcooling on T_{rw} is remarkable and growing. For the high subcooling of 80K, T_{rw} occurs nearby to T_i. As T_i increases T_{rw} rises. Therefore, higher T_i and/or higher subcooling lead to higher T_{rw}. Since, there is no correlation for water jet quenching on steel surface available in literature to predict T_{rw}, taking into account the influence of T_i, subcooling, and V_j, an empirical correlation (Eq. 1) based on present results, has been proposed

$$T_i - T_{rw} = \frac{22563}{\Delta T_{sub}^{1.44} V_j^{0.09}} \left(\frac{T_i - 450}{450 - T_{sat}} \right)^3 \quad (1)$$

Figure 9-b shows the comparison between experimental and predicted T_{rw} by Eq. (1). The predicted values have presented a standard deviation (σ) of ± 7.6°C (95% confidence) from observed data in present study.

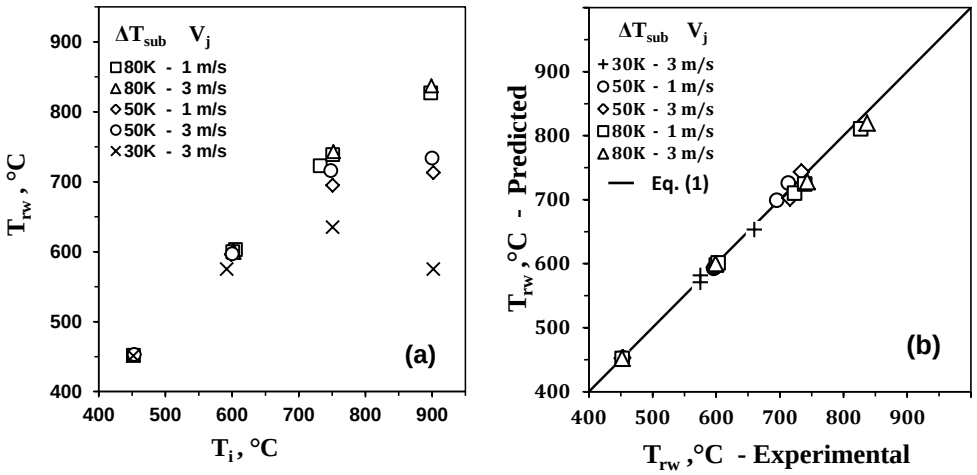

(a) Effect of T_i, subcooling, and jet velocity on rewetting temperature.

(b) Comparison of experimental T_{rw} and predicted T_{rw} by Eq. (1).

Figure 9. Rewetting temperature as function of T_i, subcooling, and jet velocity.

3.2. Rewetting delay

Figure 10-a shows the effect of T_i, jet velocity, and subcooling on rewetting delay (t_{rw}). The data evidence t_{rw} is a strong function of subcooling and T_i, and, less intense, of V_j. Rewetting delay is enlarged as T_i rises and subcooling reduces. Correlations to predict t_{rw} in jet quenching are scarce in literature and they are not applicable for the test conditions of the present study. Hence, an empirical correlation (Eq. 2), within 95% of confidence, has been proposed

$$t_{rw} = 0.00156\ exp\left[\frac{T_i(39.3 - 2.1\ V_j)0.00094}{\Delta T_{sub}^{0.421}}\right] \quad (2)$$

The predicted values have presented a standard deviation (σ) of ± 0.012 s (95% confidence) from observed data in present study (Figure 10-b).

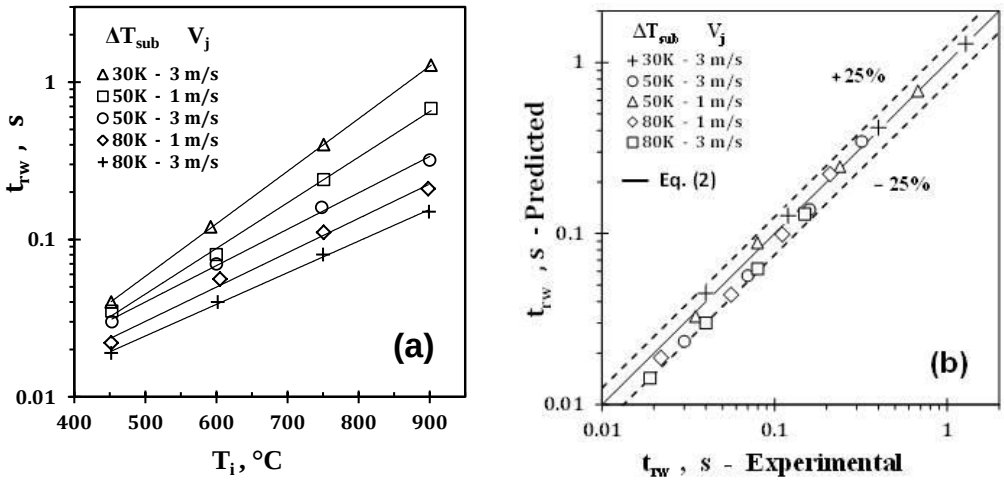

Figure 10. (a) Effect of T_i , subcooling and jet velocity on rewetting delay (t_{rw}); (b) Comparison of experimental and predicted t_{rw} by Eq. (2).

3.4. Cooling curves

Cooling curve with corresponding flow patterns and boiling regimes are shown in Figure 11 for T_i = 751°C, ΔT_{sub} = 80K and V_j = 1 m/s. Images A through to E show the successive stages of flow boiling regimes with names that denote the most striking feature: film boiling, transition, maximum heat flux, nucleate boiling, and single-phase flow. Film boiling still occurs on the surface 0.02 s after quenching has started (image A) and the surface temperature, T_s, of 751°C remains about unaltered due to the low heat transfer across vapor layer.

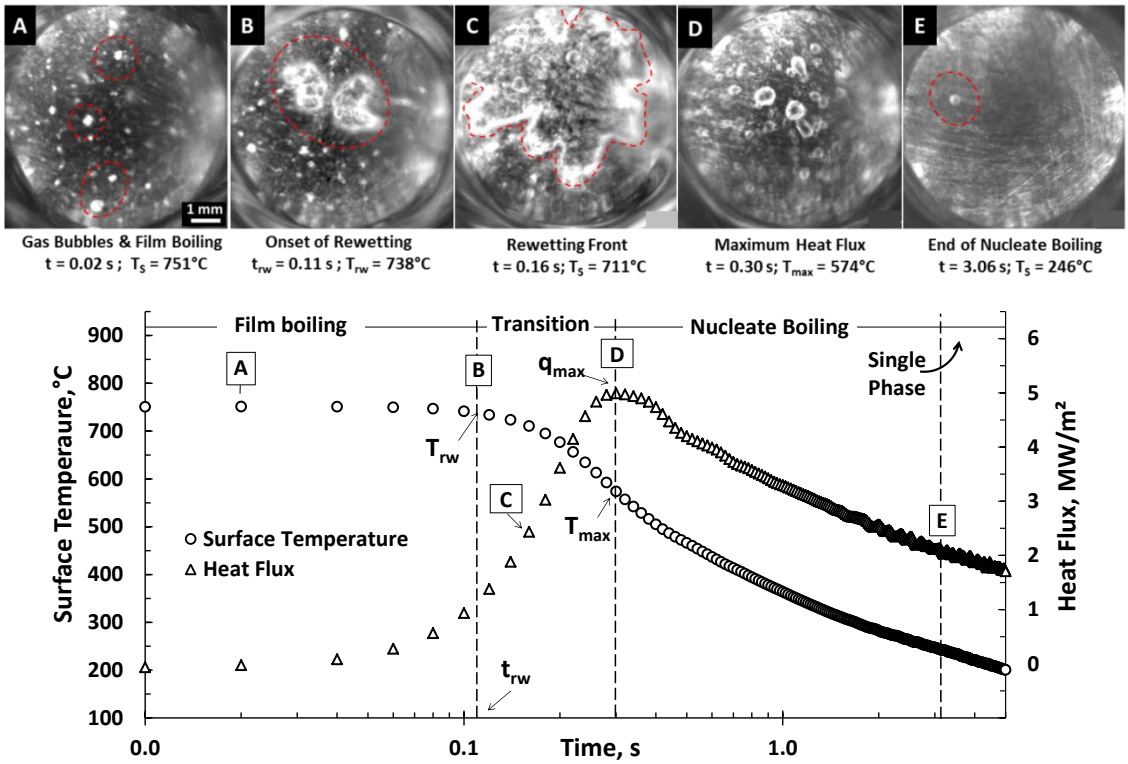

Figure 11. Heat transfer and boiling regimes in jet impingement quenching for T_i = 751°C, ΔT_{sub} = 80K, and jet velocity of 1 m/s.

The red dashed circles in Figure 11 highlight some of many gas bubbles present during film boiling. Rewetting occurs at t_{rw} = 0.11 s when surface temperature, T_s, is 738°C where two wetted spots (red dashed circles) are seen in image B. Note that rewetting did not occur at the time of a sharp rise in heat flux but later already at a time when the rewetting heat flux (q_{rw}) is 1.1 MW/m².

Image C shows the wetted area increasing with the advancement of the rewetting front outwards (red dashed line). Intense bubbly activity is observed within the wetted area while outside this area the gas bubbles still remain on top of the vapor film, with T_s = 711°C and q_s = 2.4 MW/m². The maximum heat flux, q_{max}, of 5.0 MW/m² occurs at t = 0.30 s and T_s = 574°C (image D) and marks the beginning of a nucleate boiling regime where the heat flux curve slope becomes negative. A gradual reduction in bubble population is observed until the bubbly activity ceases (Image E) at t = 3.06 s, for T_s = 246°C and q_s = 2.1 MW/m². The high subcooling of 80K seems to be the main reason for ceasing the bubbly activity on surface at 246°C.

4. CONCLUSIONS

The characterization of rewetting phenomenon in water jet quenching of high temperature steel plate was achieved with the aid of a novel high speed imaging technique. For the first time, gas bubbles from degassing have been observed on top of a vapor film. Roughness and surface induce rewetting occurs on surface above the critical point of water. Rewetting occurs on top of those asperities and act as microfins on hot surface. For initial surface temperatures at or below 300°C rewetting occurs without a vapor film. For initial surface temperature at or above 450°C film boiling occurs even for high subcooling of 80K. In both cases, intense bubbly activity was observed in wetted area. High subcooling and jet velocity cannot suppress bubbly activity on surface at or above 300°C. Data suggest that a stable solid-liquid contact is bound to occur on surface at or below thermodynamic limit of liquid superheat. Temperature and time of rewetting are strongly affected by the initial surface temperature and jet subcooling and, less intensely, by jet velocity. Higher initial temperature and/or higher jet subcooling lead to higher rewetting temperatures.

REFERENCES

1 V. Carey, Liquid–Vapor Phase-Change Phenomena, Second Edition ed., New York: Taylor & Francis, 2007.

2 J. H. Lienhard, N. Shamsundar e P. O. Biney, “Spinodal lines and equations of state: a review,” Nuclear Engineering and Design, vol. 95, pp. 297-314, 1986.

3 D. Hall, F. Incropera e R. Viskanta, “Jet Impingement Boiling From a Circular Free-Surface Jet During Quenching: Part 1 - Single-Phase Jet,” ASME Journal of Heat Transfer, vol. 123, n. 5, pp. 901-910, 2001.

4 S. Ishigai, S. Nakanish e T. Ochi, “Boiling heat transfer for a plane water jet impinging on a hot surface,” em Proceedings 6th Int. Heat Transfer Conference, Toronto, Canada, 1978.

5 T. Ochi, S. NakanishI e M. I. S. Kaji, “Cooling of a hot plate with an impinging circular water jet,” em Multi-Phase Flow and Heat transfer III. Part A: Fundamentals, Amsterdam, 1984.

6 J. Filipovic, F. P. Incropera e R. Viskanta, “Rewetting temperature and velocity in a quenching experiment,” Experimental Heat Transfer, vol. 8, n. 4, p. 257–270, 1995.

7 P. L. Woodfield, M. Monde e A. K. Mozumder, “Observations of high temperature impinging-jet boiling phenomena,” International Journal of Heat and Mass Transfer, vol. 48, n. 10, p. 2032–2041, 2005.

8 M. Ilyas, M. Ahmad, C. P. Hale, S. P. Walker e G. F. Hewitt, “Rewetting Processes During Top/Bottom Re-Flooding of Heated Vertical Surfaces,” em ASME/JSME 2011 8th Thermal Engineering Joint Conference, Honolulu, Hawaii, 2011.

9 H. Ohtake e Y. Koizumi, “Study on propagative collapse of a vapor film in film boiling (mechanism of vapor-film collapse at wall temperature above the thermodynamic limit of liquid superheat),” International Journal of Heat and Mass Transfer, vol. 47, n. 8-9, p. 1965–1977, 2004.

10 M. N. Hasan, M. Monde e Y. Mitsutake, “Homogeneous nucleation boiling during jet impingement quench of hot surfaces above thermodynamic limiting temperature,” International Journal of Heat and Mass Transfer, vol. 54, p. 2837–2843, 2011.

11 F. Xu e M. Gadala, “Heat transfer behavior in the impingement zone under circular water jet,” International Journal of Heat and Mass Transfer, vol. 49, p. 3785–3799, 2006.

12 Z. Liu e J. Wang, “Study on film boiling heat transfer for water jet impinging on high temperature flat plate,” International Journal of Heat and Mass Transfer, vol. 44, pp. 2475-2481, 2001.

13 C. Agrawal, R. Kumar and A. Gupta, "Rewetting and maximum surface heat flux during quenching of hot surface by round water jet impingement," International Journal of Heat and Mass Transfer, vol. 55, p. 4772–4782, 2012.
14 S. G. Lee, M. Kaviany, C. Kim e L. Lee, “Quasi-steady front in quench subcooled-jet impingement boiling: Experiment and analysis,” International Journal of Heat and Mass Transfer, vol. 113, p. 622–634, 2017.
15 N. Karwa e P. Stephan, “Experimental investigation of free-surface jet impingement quenching process,” International Journal of Heat and Mass Transfer, vol. 64, p. 1118–1126, 2013.
16 B. Wang, X. Guo, Q. Xie, Z. Wang e G. Wang, “Heat transfer characteristics during jet impingement on a high-temperature plate surface,” Applied Thermal Engineering, vol. 100, p. 902–910, 2016.
17 K. Takrouri, J. Luxat e M. Hamed, “Experimental investigation of quench and re-wetting temperatures of hot horizontal tubes well above the limiting temperature for solid–liquid contact,” Nuclear Engineering and Design, vol. 311, p. 167–183, 2017.
18 B. Piggott, E. White e R. DuffeyY, “Wetting delay due to film and transition boiling on hot surfaces,” Nuclear Engineering and Design, vol. 36, pp. 169-181, 1976.
19 A. K. Mozumder, M. Monde e P. L. Woodfield, “Delay of wetting propagation during jet impingement quenching for a high temperature surface,” International Journal of Heat and Mass Transfer, vol. 48, p. 5395–5407, 2005.
20 F. P. Incropera, D. DeWitt, T. L. Bergman e A. S. Lavine, Fundamentals of Heat and Mass Transfer, 7th ed., John Wiley & Sons, 2011.
21 J. Taylor, An Introduction to Error Analysis – The Study of uncertainties in physical measurements, Second Edition ed., University of Colorado, 1996.
22 H. Leocadio, J. Passos e A. Silva, “Heat transfer behavior of a high temperature steel plate cooled by a subcooled impinging circular water jet,” em 7th ECI International Conference on Boiling Heat Transfer, Florianopolis, 2009.
23 S. V. Ravikumar, J. M. Jha e I. Sarkar, “Mixed-surfactant additives for enhancement of air-atomized spray cooling of a hot steel plate,” Experimental Thermal and Fluid Science, vol. 55, p. 210–220, 2014.
24 A. Ahmed e M. Hamed, “Modeling of transition boiling under an impinging water jet,” International Journal of Heat and Mass Transfer, vol. 91, p. 1273–1282, 2015.
25 N. Karwa, L. Schmidt e P. Stephan, “Hydrodynamics of quenching with impinging free-surface jet,” International Journal of Heat and Mass Transfer, vol. 55, p. 3677–3685, 2012.